Lévy flights in an infinite potential well as a hypersingular Fredholm problem

Elena V. Kirichenko, Piotr Garbaczewski, Vladimir Stephanovich, and Mariusz Żaba
Faculty of Mathematics, Physics and Informatics, University of Opole, 45-052 Opole, Poland
(Received 18 January 2016; revised manuscript received 3 April 2016; published 5 May 2016)

We study Lévy flights with arbitrary index $0 < \mu \leqslant 2$ inside a potential well of infinite depth. Such a problem appears in many physical systems ranging from stochastic interfaces to fracture dynamics and multifractality in disordered quantum systems. The major technical tool is a transformation of the eigenvalue problem for initial fractional Schrödinger equation into that for Fredholm integral equation with hypersingular kernel. The latter equation is then solved by means of expansion over the complete set of orthogonal functions in the domain D, reducing the problem to the spectrum of a matrix of infinite dimensions. The eigenvalues and eigenfunctions are then obtained numerically with some analytical results regarding the structure of the spectrum.

DOI: 10.1103/PhysRevE.93.052110

I. INTRODUCTION

To describe the complex behavior of disordered systems without using Gaussian approximation, the stochastic processes, called Lévy flights, are commonly utilized [1–3]. The stochastic trajectories of Lévy flights alternate between some continuous motions and jumps (sometimes extremely long) and hence do not obey Gaussian statistics [4–6]. The length of these jumps obeys to so-called Lévy stable distributions with power-law tails, which decay much slower then Gaussian ones. This yields the divergence of already second moment of such distributions. Contrary to ordinary diffusion, described by Gaussian distributions, the above jump-type discontinuous motions are commonly attributed as anomalous diffusion [5,6]. It turns out that Lévy stable distributions and Lévy flights are relevant to many physical [7–11], chemical, biological [12–14], and socioeconomic [15–17] systems. Prominent physical examples are subrecoil laser cooling of trapped atoms [10], energy exchange in Landau-Teller model of molecular collisions [11], and so-called multifractality of the wave functions in the disordered quantum systems [18,19].

It is well known that the concentration $n(x,t)$ of particles performing Lévy flights satisfies in its simplest form a diffusion equation where the Laplacian operator is replaced by a fractional derivative,

$$\frac{\partial n(x,t)}{\partial t} = -|\Delta|^{\mu/2} n(x,t), \tag{1}$$

where $|\Delta|^{\mu/2}$ (Lévy index $0 < \mu \leqslant 2$) is a fractional Laplacian of order $\mu/2$, restricted to 1D case [20] so that at $\mu = 2$ we recover the ordinary Laplace operator [21,22]. The explicit form of this operator reads

$$|\Delta|^{\mu/2} f(x) = -A_\mu \int_R \frac{f(u) - f(x)}{|u - x|^{1+\mu}}\, du, \tag{2}$$

$$A_\mu = \frac{\Gamma(\mu + 1)\sin(\pi\mu/2)}{\pi}, \tag{3}$$

which shows that this operator is spatially nonlocal, becoming an issue if confronted with *a priori* imposed boundary conditions. This is irrespective of whether we are interested in Lévy processes with absorption (killing) at the boundaries or in so-called fractional quantum mechanics.

Namely, at the unbounded domains, the fractional Laplacian Eq. (2) is most easily defined by its Fourier transform

$$\frac{1}{2\pi}\int_{-\infty}^{\infty} |k|^\mu f(k) e^{-\imath kx} dk \equiv -\frac{\partial_\mu f(x)}{\partial |x|^\mu} = |\Delta|^{\mu/2} f(x), \tag{4}$$

while on bounded domains $D \subset R$ (R is a real axis) the Fourier transform Eq. (4) is no longer operational [23–29]; see specifically Refs. [25,26]. Transformation Eq. (4) permits us to solve many problems related to fractional diffusion and fractional quantum mechanics in k space on unbounded domains [5,30,31], while on the bounded ones this method fails, making the problem nontrivial.

In this paper, we investigate the Lévy flights of arbitrary index $0 < \mu \leqslant 2$ confinement by the infinite potential well, which arises naturally in the context of so-called first-passage problems [32,33]. We show that this problem is equivalent to that of fractional quantum mechanics of a particle in a potential well of infinite depth [34,35]. We solve this problem by further reducing the corresponding fractional Schrödinger equation to the Fredholm integral equation with hypersingular kernel. The latter equation has been solved with arbitrary accuracy (for eigenstates and eigenfunctions) by the expansion over the (infinite) complete set of orthogonal functions, which in the case of above potential well are trigonometric functions. This expansion is suitable for any Lévy index $0 < \mu \leqslant 2$, although many results are obtained for so-called ultrarelativistic or Cauchy case $\mu = 1$. This case corresponds to zero mass ($m = 0$) case of the relativistic Hamiltonian $\mathcal{H} = \sqrt{-\hbar^2 c^2 \Delta + m^2 c^4} - mc^2$ (c is the velocity of light, Δ is ordinary Laplacian), and thus is physically sound [24–28]. Note also purely mathematical literature [29,36–40] in the context of the case $\mu = 1$. We show that our algorithm, consisting in the expansion of the solution over the suitable set of orthogonal functions, permits us to attack successfully virtually any problem of so-called fractional quantum mechanics.

II. FREDHOLM INTEGRAL EQUATION FOR THE SPECTRUM

We consider the fractional Scrödinger equation,

$$\left[-|\Delta|^{\mu/2} + V(x)\right]\psi(x) = E\psi(x), \tag{5}$$

 ©2016 American Physical Society

where

$$V(x) = \begin{cases} 0, & x \in [-1,1] \\ \infty, & \text{otherwise}, \end{cases} \tag{6}$$

which implies that $\psi(x) = 0$ for $|x| \geqslant 1$ and defines the infinitely high "walls" of the potential well in the points $x = \pm 1$. Now, the whole real axis R can be divided into the regions inside $-1 \leqslant x \leqslant 1$ and outside well Eq. (6) to get

$$\begin{aligned} |\Delta|_D^{\mu/2}\psi(x) &= -A_\mu \int_{-\infty}^{\infty} \frac{\psi(u)-\psi(x)}{|u-x|^{1+\mu}}du \\ &= -A_\mu \left[\int_{-\infty}^{-1} + \int_{-1}^{1} + \int_{1}^{\infty}\right] \frac{\psi(u)-\psi(x)}{|u-x|^{1+\mu}}du. \end{aligned} \tag{7}$$

The symbolic integration signs in the square brackets in Eq. (7) mean the sum of corresponding integrals. Now we make note of the fact that for regions outside the well $\psi(u) = 0$, so that we have

$$\begin{aligned} |\Delta|_D^{\mu/2}\psi(x) &= -A_\mu \int_{-1}^{1} \frac{\psi(u)du}{|u-x|^{1+\mu}} + \Delta I_\mu, \\ \Delta I_\mu &= A_\mu \psi(x) \left[\int_{-\infty}^{-1} + \int_{-1}^{1} + \int_{1}^{\infty}\right] \frac{du}{|u-x|^{1+\mu}}. \end{aligned} \tag{8}$$

It can be shown that with respect to definition of modulus ($|u-x| = u-x$ if $u > x$ and $x-u$ if $u < x$) and above division of real axis R into three subintervals, the integral ΔI_μ is defined by the values of antiderivative at infinities. These values are zero except the case $\mu = 0$, where they are logarithmically divergent. This yields $\Delta I_\mu \equiv 0$ for $0 < \mu \leqslant 2$, so that the desired integral equation acquires the form

$$-A_\mu \int_{-1}^{1} \frac{\psi(u)du}{|u-x|^{1+\mu}} = E\psi(x). \tag{9}$$

Equation (9) is the Fredholm integral equation, which we are going to solve below. We will show that at $\mu = 2$ our solution recovers the case of the infinite potential well with ordinary Laplacian [41]. Note that for $\mu = 1$ the integral in Eq. (9) refers to the so-called Hadamard finite part of singular integrals, extensively employed in the works of crack propagation in solids [37–40,42–45].

Note also that the spectral problem Eq. (9) is the homogeneous Fredholm equation with a hypersingular symmetric kernel $K(t,x) = A_\mu|u-x|^{-1-\mu}$. If the kernel of Eq. (9) is nonsingular (i.e., such that $\int_a^b \int_a^b K^2(x,t)dxdt < \infty$), then this equation obeys so-called Fredholm alternative [46]: either E [or $\lambda = 1/(\pi E)$] is its eigenvalue and ψ is eigenfunction or the equation has a trivial solution $\psi(x) = 0$. Also, for nonsingular kernel, the number of eigenstates is discreet and finite [46] and exactly for Eq. (9) with nonsingular kernel its eigenfunctions are $\sin(n\pi x)$ and $\cos(n\pi x/2)$; i.e., they correspond to the case of infinite well in ordinary quantum mechanics [41]. On the other hand, for the case of singular kernels, the solution of the spectral problem (if in existence) has an infinite (although discreet) number of eigenstates [46].

One more remark is in place here. As we will see below, the best way to solve the integral Eq. (9) is to expand its solution over the complete set of orthogonal functions. In our view, the best choice of such a set is the eigenfunctions of the corresponding ordinary (i.e., that with ordinary Laplacian) quantum mechanics. In other words, we can claim that the fractional derivative in corresponding quantum mechanical problem "mixes" all the eigenstates of that with ordinary Laplacian. This means, for instance, that even ground-state wave function for $\mu \neq 2$ is indeed an infinite superposition of the functions, corresponding to $\mu = 2$. Below we are going to realize this algorithm.

III. THE SOLUTION OF THE INTEGRAL EQUATION

Now we are going to solve the integral Eq. (9), i.e., to deduce the eigenfunctions and eigenvalues of the nonlocal operator $|\Delta|_D^{\mu/2}$. As we have mentioned above [46], there are no systematic methods (even numerical) of solution of integral equations with singular (or hypersingular) kernels. Along the lines of the above scenario, below we suggest an effective algorithm of such solution, based on the "mixture" of the quantum states of the infinite potential well with ordinary Laplacian, i.e., that for $\mu = 2$. More precisely, we are looking for the solution as an expansion over the appropriate complete set of orthogonal functions, which in our case turn out to be trigonometric Fourier series. Our algorithm permits us to obtain the eigenfunctions and eigenvalues of the problem Eq. (9) with arbitrary accuracy by reducing it to the eigenproblem of the infinite matrix. Our method also permits us to obtain approximate analytical expressions for eigenvalues and several first eigenfunctions.

Our algorithm is based on the following assumptions:

(1) Based on standard quantum mechanical infinite well experience [41] and previous attempts to solve the Lévy-stable infinite well problem ([38,39] and [24–26]), we can safely classify eigenfunctions to be odd or even. The oscillation theorem [41] appears to be valid here so that the ground-state wave function has no nodes (intersections with x axis), first excited state has one node, second one has two nodes, etc. So, our even states can be labeled by quantum numbers $k = 0, 2, 4, 6,...$ while odd states by $k = 1, 3, 5,....$

(2) Similar to ordinary quantum mechanics [41], the Hilbert space of the system can be interpreted as a direct sum of odd and even subspaces, equipped with corresponding orthonormal sets of functions in the interval $[-1,1]$.

(3) As the complete set of eigenfunctions of the ordinary ($\mu = 2$) infinite well [41] consists of standard trigonometric functions, we will look for the eigenfunctions of the problem Eq. (9) in the form of trigonometric series.

(4) The even basis system in $L^2(D)$ is composed of cosines,

$$\varphi_k(x) = \cos\frac{(2k+1)\pi x}{2}, \quad \int_{-1}^{1} \varphi_k(x)\varphi_l(x)dx = \delta_{kl}, \quad k \geqslant 0, \tag{10}$$

where δ_{kl} is the Kronecker δ. For the odd basis system we take the sines

$$\chi_k(x) = \sin k\pi x, \quad \int_{-1}^{1} \chi_k(x)\chi_l(x)dx = \delta_{kl}, \quad k \geqslant 1. \tag{11}$$

(5) We look for eigenfunctions of $|\Delta|_D^{1/2}$ separately in odd and even Hilbert subspaces of $L^2(D)$.

Presuming that the Fourier (trigonometric) series converge, for even functions we have

$$\psi_e(x) = \sum_{k=0}^{\infty} a_{k\mu} \cos \frac{(2k+1)\pi x}{2}, \tag{12}$$

while for odd functions

$$\psi_o(x) = \sum_{k=1}^{\infty} b_{k\mu} \sin k\pi x. \tag{13}$$

To avoid confusion, we point out that the standard numbering of overall infinite well eigenfunctions begins with $n = 1$ rather then from $k = 0$ (even case) or $k = 1$ (odd case) as we have assumed above. We need to have a clear discrimination between sine (odd) and cosine (even) Fourier series expansions. The final outcomes will be relabeled in terms of consecutive integers $n = 1,2,....$

A. Even subspace

In this case we substitute the function $\psi_e(x)$ Eq. (12) into Eq. (9) to obtain

$$\sum_{k=0}^{\infty} a_{k\mu} f_{k\mu}(x) = E \sum_{k=0}^{\infty} a_{k\mu} \cos \frac{(2k+1)\pi x}{2}, \tag{14}$$

where

$$f_{k\mu}(x) = -A_\mu \int_{-1}^{1} \frac{\cos \frac{(2k+1)\pi u}{2}}{|u-x|^{1+\mu}} du. \tag{15}$$

It can be shown that the integrals in Eq. (15) are convergent for any $0 < \mu \leqslant 2$. They can be exactly reduced to the form, which does not contain removable divergences,

$$\begin{aligned} f_{k\mu}(x) = -\frac{A_\mu \lambda_k^\mu}{\mu} \Bigg\{ & \sin \lambda_k x \int_{\lambda_{k-}}^{\lambda_{k+}} u^{-\mu} \cos u \, du \\ & - \cos \lambda_k x \Bigg[\int_0^{\lambda_{k-}} u^{-\mu} \sin u \, du \\ & + \int_0^{\lambda_{k+}} u^{-\mu} \sin u \, du \Bigg] \Bigg\}, \\ \lambda_k = \frac{\pi}{2}(2k+1),\ & \lambda_{k\pm} = \lambda_k(1 \pm x). \end{aligned} \tag{16}$$

Note that the integrals in square brackets of Eq. (16) are convergent at $u = 0$ for all $0 < \mu < 2$ [we have integrable feature like $\int u^{1-\mu} du = u^{2-\mu}/(2-\mu)$], while the divergence at $\mu = 2$ is compensated by zero of $A_{\mu\to 2} = 2 - \mu$.

Equation (16) permits us to represent functions $f_{k1}(x)$ at $\mu = 1$ through sine [Si(x)] and cosine [Ci(x)] integral functions [47,48],

$$\begin{aligned} f_{k1}(x) = \frac{\lambda_k}{\pi} \{ & \sin \lambda_k x [\mathrm{Ci}\ \lambda_{k-} - \mathrm{Ci}\ \lambda_{k+}] \\ & + \cos \lambda_k x [\mathrm{Si}\ \lambda_{k-} + \mathrm{Si}\ \lambda_{k+}] \}. \end{aligned} \tag{17}$$

Note that some integrals in Eq. (16) as well as the functions Ci$\lambda_{k\pm}$ are singular at $x \to \pm 1$ [48]. Nonetheless, this singularity turns out to be removable by subsequent integration with $\varphi_k(x)$, Eq. (10), so that the resulting matrix elements are finite; see below.

Now we multiply both sides of Eq. (14) by $\varphi_i(x)$, Eq. (10), and integrate from -1 to 1 with respect to the orthonormality of $\varphi_i(x)$. Equation (14) is now replaced by an (infinite) matrix eigenvalue problem,

$$\begin{aligned} & \sum_{i,k=0}^{\infty} a_{k\mu} \gamma_{\mu ki} = E a_{i\mu}, \\ & \gamma_{\mu ki} = \int_{-1}^{1} f_{k\mu}(x) \varphi_i(x) dx,\ i,k,l = 0,1,2,3,..., \end{aligned} \tag{18}$$

whose approximate solution can be done considering successive eigenvalue problems for finite $n \times n$ matrices. Note that the expressions for diagonal matrix elements $\gamma_{\mu ii}$ give already good approximation for corresponding eigenvalues, especially for large i.

The set Eq. (18) is a linear homogeneous system, which, according to Kronecker-Capelli theorem, has a nontrivial solution only if its determinant equals zero. This permits us to determine the eigenvalues $E_{k\mu}$ and the coefficients $a_{k\mu}$ of the expansion Eq. (10) as the eigenvectors, corresponding to each $E_{k\mu}$. We calculate the integrals $\gamma_{\mu ki}$ numerically, but it turns out that some of them (for instance, the diagonal elements γ_{1ii} at $\mu = 1$) can be evaluated analytically. The explicit forms of $f_{k\mu}(x)$ [Eq. (16)] and $\varphi_i(x)$ [Eq. (10)] show that the matrix Eq. (18) is symmetric, i.e., $\gamma_{\mu ki} = \gamma_{\mu ik}$, which means that eigenvalues are real.

We have for diagonal elements at $\mu = 1$,

$$\gamma_{1kk} = -\frac{2}{\pi} + (2k+1)\mathrm{Si}[\pi(2k+1)], \tag{19}$$

while for couple of first nondiagonal elements γ_{1ki}:

$$\begin{aligned} \gamma_{10} &= \frac{6\mathrm{Ci}(\pi) - 6\mathrm{Ci}(3\pi) + \ln 729}{8\pi} = 0.2773259, \\ \gamma_{20} &= -\frac{5}{24\pi}(2\mathrm{Ci}(\pi) - 2\mathrm{Ci}(5\pi) + \ln 25) = -0.2227035, \\ \gamma_{21} &= \frac{5}{16\pi}(6\mathrm{Ci}(3\pi) - 6\mathrm{Ci}(5\pi) + \ln \frac{15625}{729}) = 0.3088509, \end{aligned} \tag{20}$$

where for clarity we suppress first index $\mu = 1$.

The explicit form of the matrix Eq. (18) reads (for each μ; we once more suppress this index)

$$\hat{A}_D = \begin{pmatrix} \gamma_{00} & \gamma_{10} & \cdots & \gamma_{n0} \\ \gamma_{10} & \gamma_{11} & \cdots & \gamma_{n1} \\ \vdots & \cdots & \cdots & \vdots \\ \gamma_{n0} & \gamma_{n1} & \cdots & \gamma_{nn} \end{pmatrix}. \tag{21}$$

To find its eigenvalues and eigenvectors we use iterative procedure, considering partial matrices 2×2, 3×3 etc. The eigenvalues of the simplest partial matrix 2×2 give the lowest order approximation of ground state and *second* excited state $n = 2$. The equation for associated eigenvalues reads

$$\begin{vmatrix} \gamma_{00} - E & \gamma_{10} \\ \gamma_{10} & \gamma_{11} - E \end{vmatrix} = 0. \tag{22}$$

The analytical expressions for E_0 and E_2 can be obtained by means of analytical formulas for γ_{ik} [Eqs. (19) and (20)]. Although computations are cumbersome, one arrives at a reasonable (albeit still far form being sharp) approximation to eigenvalues associated with the ground state and second (or first even) excited state. Using numerical values of γ_{1ik}, Eq. (18), we calculate for $\mu = 1$,

$$E_0 = 1.191256,\ E_2 = 4.411727; \tag{23}$$

$$\begin{aligned}\psi(E_0) &= (-0.996257,\ 0.086437),\\ \psi(E_2) &= (0.086437,\ 0.996257),\end{aligned} \tag{24}$$

where $\psi(E_0)$ are eigenvectors, corresponding to eigenvalues E_0 and E_2. In other words, the approximate (crude, low-order) shapes of the eigenfunctions read

$$\psi_0 = -0.996257\cos\frac{\pi x}{2} + 0.086437\cos\frac{3\pi x}{2}, \tag{25}$$

$$\psi_2 = 0.086437\cos\frac{\pi x}{2} + 0.996257\cos\frac{3\pi x}{2}, \tag{26}$$

where $\psi_0(x)$ and $\psi_2(x)$ correspond to ground and second excited state. We note here that the reproduced eigenvectors are $L^2(D)$ normalized, while an overall sign may be negative. Latter is not important as the physically meaningful quantity is $|\psi|^2$.

The same procedure yields for $\mu = 0.5$:

$$E_0 = 0.995534,\ E_2 = 2.06879; \tag{27}$$

$$\begin{aligned}\psi(E_0) &= (-0.991128,\ 0.132914),\\ \psi(E_2) &= (0.132914,\ 0.991128),\end{aligned} \tag{28}$$

and for $\mu = 1.7$

$$E_0 = 1.89053,\ E_2 = 13.4318; \tag{29}$$

$$\begin{aligned}\psi(E_0) &= (-0.999647,\ 0.0265864),\\ \psi(E_2) &= (0.0265864,\ 0.999647).\end{aligned} \tag{30}$$

It is seen that with increase of μ the ground-state energy decreases, while the difference between ground and excited states increases. Also, for decreased μ the situation is opposite. Below we investigate this question in more detail.

By increasing the matrix order from 2 to 3, we improve the accuracy with which lowest states are reproduced and increase their number by one. For $\mu = 1$ we have for eigenenergies,

$$E_0 = 1.1814891,\ E_2 = 4.3854565,\ E_4 = 7.569241. \tag{31}$$

It is seen that while one more state appears, numerical outcomes for lowest states are corrected by approximately 1%. This statement is valid for all $0 < \mu \leqslant 2$.

For the 6×6 matrix and $\mu = 1$ we have

$$\begin{aligned}&E_0 = 1.1704897,\ E_2 = 4.35648331,\\ &E_4 = 7.52132,\ E_6 = 10.68291,\\ &E_8 = 13.845025,\ E_{10} = 17.01393.\end{aligned} \tag{32}$$

At the same time for $\mu = 1.7$,

$$\begin{aligned}&E_0 = 1.88345,\ E_2 = 13.394,\\ &E_4 = 32.4753,\ E_6 = 57.9598,\\ &E_8 = 89.2117,\ E_{10} = 125.814.\end{aligned} \tag{33}$$

It is interesting to confront the above obtained (still crude) approximate eigenvalues with analytical expression, obtained in Ref. [38] (see also Ref. [39]),

$$E_{n\mu} \approx \left[\frac{n\pi}{2} - \frac{(2-\mu)\pi}{8}\right]^{\mu}, \quad n = 1,2,3,... \tag{34}$$

Table I shows such comparison for three representative values of μ. It it seen a very good (with the accuracy less then 1%) coincidence between numerical values (obtained from not small-sized 6×6 matrix) and those from Eq. (34). This already demonstrates the accuracy of our method for arbitrary μ.

Obviously, while passing to higher order matrices the obtained solutions give better approximations to the "true" eigenvalues and eigenvectors of the infinite well problem. The analysis of numerical values of matrix elements in Eq. (21) shows that for any μ these of diagonal elements are much larger than the off-diagonal ones. This difference appears to be lowest for γ_{00}. For larger k the diagonal elements grow (for instance at $\mu = 1$ $\gamma_{22} \approx 4.388$), while off-diagonal values are close to 0.3. This means that diagonal elements give a fairly good approximation for eigenvalues of the matrix Eq. (21); see the first row of Table II.

B. Odd subspace

We look for eigenfunctions in the form of Eq. (13). Repeating the same steps as for the even subspace we generate

TABLE I. The comparison of six lowest even eigenvalues E_i for different μ obtained numerically from 6×6 matrix and from approximate Eq. (34).

i	0	2	4	6	8	10
$\mu = 0.5$, Num.	0.97976	2.04538	2.71443	3.24759	3.70492	4.11305
$\mu = 0.5$, Ex. (34)	0.990832	2.0306	2.69535	3.22591	3.68078	4.0853
$\mu = 1.0$, Num.	1.1704897	4.35648331	7.52131594	10.68291	13.845025	17.01393
$\mu = 1.0$, Ex. (34)	1.1781	4.31969	7.46128	10.6029	13.7445	16.8861
$\mu = 1.7$, Num.	1.88345	13.394	32.4753	57.9598	89.2117	125.814
$\mu = 1.7$, Ex. (34)	1.88732	13.3603	32.3962	57.8252	89.0098	125.522

TABLE II. Comparative table of six lowest eigenvalues E_i in the Cauchy infinite potential well, $\mu = 1$. Results for matrices of different sizes in our approach are compared with spectral data of Refs. [38,39] and [24,26]. First six diagonal elements of the matrix Eq. (21) [Eqs. (19) and (38), respectively] are cited for comparison. Note that the numbering of states follows tradition ($i = 1, 2, 3, 4, 5, 6$) and refers to consecutive eigenvalues, with no reference to the parity of respective eigenfunctions.

i	1	2	3	4	5	6
Diagonal elem.	1.21531728	2.83630315	4.38766562	5.96864490	7.53320446	9.10820377
E_{i6x6}	1.1704897	2.780209	4.356483317	5.9397942	7.52131594	9.099426
E_{i12x12}	1.1644016	2.7690111	4.3388792	5.919976	7.4952827	9.0725254
$E_{i10^4x10^4}$	1.157791	2.754795	4.3168638	5.892233	7.460284	9.032984
$E_{i(K)}$[38] Table II	1.1577	2.7547	4.3168	5.8921	7.4601	9.0328
$E_{i(KKMS)}$[39] Eq. (11.1)	1.1577738	2.7547547	4.3168010	5.8921474	7.4601757	9.0328526
$E_{i(ZG)}$[24] Table VII	1.1560	2.7534	4.3168	5.8945	7.4658	9.0427
$E_{i(zg)}$ [26] Table III	1.157776	2.754769	4.316837	5.892214	7.460282	*

the following set of equations:

$$\sum_{i,k=1}^{\infty} b_{k\mu}\eta_{\mu ki} = Eb_{l\mu}, \quad \eta_{\mu ki} = \int_{-1}^{1} g_{k\mu}(x)\chi_i(x)dx,$$
$$i,k,l = 1,2,3,..., \tag{35}$$

$$g_{k\mu}(x) = -A_\mu \int_{-1}^{1} \frac{\sin k\pi u}{|u-x|^{1+\mu}}du$$
$$= \frac{A_\mu b_k^\mu}{\mu}\left\{\cos b_k x \int_{b_{k-}}^{b_{k+}} u^{-\mu}\cos u du\right.$$
$$\left. + \sin b_k x\left[\int_0^{b_{k-}} u^{-\mu}\sin u du + \int_0^{b_{k+}} u^{-\mu}\sin u du\right]\right\},$$
$$b_k = k\pi,\ b_{k\pm} = b_k(1 \pm x). \tag{36}$$

For $\mu = 1$ we have from Eq. (36)

$$g_{k1}(x) = k\{\sin b_k x(\mathrm{Si}\ b_{k-} + \mathrm{Si}\ b_{k+})$$
$$- \cos b_k x(\mathrm{Ci}\ b_{k-} - \mathrm{Ci}\ b_{k+})\}. \tag{37}$$

We find analytically for $\mu = 1$

$$\eta_{kk} = 2k\ \mathrm{Si}(2k\pi). \tag{38}$$

For $\mu = 1$, the solutions for the 2×2 matrix have the form

$$E_1 = 2.81019,\ E_3 = 5.99476, \tag{39}$$

$$\psi(E_1) = (-0.995891,\ 0.0905574),$$
$$\psi(E_3) = (0.0905574,\ 0.995891). \tag{40}$$

We note here that since the integrals $f_{k1}(x)$ and $g_{k1}(x)$ for $\mu = 1$ can be expressed through known special functions $\mathrm{Ci}(x)$ and $\mathrm{Si}(x)$, which have very good polynomial approximations [48], the calculations for this case are much faster (and much less computer intensive) than those for $\mu \neq 1$. That is why all calculations with very large matrices like $10\,000 \times 10\,000$ have been performed here for the case $\mu = 1$, keeping in mind that the results for $\mu \neq 1$ behave themselves qualitatively similar with matrix size growth.

Two lowest eigenvalues of the 6×6 matrix for $\mu = 1$ read $E_1 = 2.78021$, $E_3 = 5.93979$. In Table II we reproduce the remaining four eigenvalues in the 6×6 case, in a comparative vein. Namely, we display the computation outcomes for the lowest six eigenvalues, while gradually increasing the matrix size, from 6×6, 12×12 to $10\,000 \times 10\,000$. We reintroduce the traditional labeling in terms of $i = 1, 2, 3, 4, 5$, so that no explicit distinction is made between even and odd eigenfunctions. Our results are directly compared with the corresponding data obtained by other methods in Refs. [38,39] and [24,26].

In Table III we report the change of the ground state energy while increasing the matrix size from 30×30 to 10000×10000. It is seen that the third significant digit stabilizes already for 300×300 and 400×400 matrices.

C. Graphical comparison

We begin with plot of the first four eigenfunctions for representative value $\mu = 1$, reported in Fig. 1. The situation for other μ's is qualitatively similar. It is seen that the states in the Cauchy well at a rough graphical resolution level resemble those of the ordinary (deriving form the Laplacian) quantum infinite well [41]. This speaks in favor of our statement that fractional Laplacian "mixes" the states, generated by an ordinary one. The detailed analysis of the eigenfunctions shape

TABLE III. The matrix $n \times n$- "size evolution" of six lowest eigenvalues for $\mu = 1$ as n grows. $E_{\mathrm{g.s.}}$ stands for ground-state energy.

n (matrix $n \times n$)	30	50	100	200	400	1000	2000	5000	10 000
$E_{g.s.} = E_1$	1.160505	1.159428	1.158608	1.158193	1.157984	1.157858	1.157816	1.157791	1.157791
E_2	2.760953	2.758572	2.756705	2.755742	2.755252	2.754954	2.754855	2.754795	2.754795
E_3	4.326418	4.322736	4.319842	4.318343	4.317578	4.317114	4.316958	4.316864	4.316864
E_4	5.904768	5.900041	5.896238	5.894235	5.893204	5.892573	5.892361	5.892233	5.892233
E_5	7.476052	7.470114	7.465334	7.462812	7.461511	7.460714	7.460446	7.460284	7.460284
E_6	9.051406	9.044604	9.039015	9.036021	9.034462	9.033504	9.033180	9.032984	9.032984

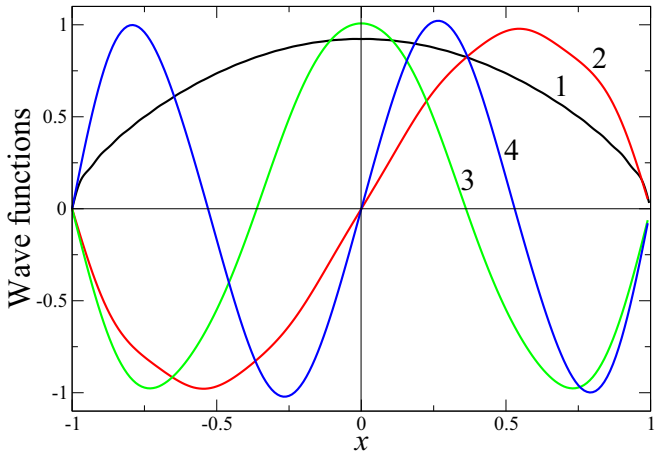

FIG. 1. Four lowest eigenfunctions in the infinite Cauchy well ($\mu = 1$), labeled $i = 1, 2, 3, 4$. Outcome of the $10^4 \times 10^4$ matrix. The qualitative behavior of the eigenfunctions for $\mu \neq 1$ is the same.

issue can be found in Ref. [26], where another method of solution of the Cauchy well problem has been tested.

Since in the present paper we employ trigonometric functions as the orthonormal basis system for low-sized matrices, Eq. (21), we deal with visually distinguishable oscillations. These are gradually smoothed with the growth of the matrix size. It is instructive to compare approximate shapes of the ground-state wave function, obtained by the diagonalization of different-sized matrices. The left panel of Fig. 2 reports the pertinent shapes in case of 3×3, 5×5, and 30×30 matrices for $\mu = 1$. We note that the qualitative features of the ground-state function approximants are practically the same

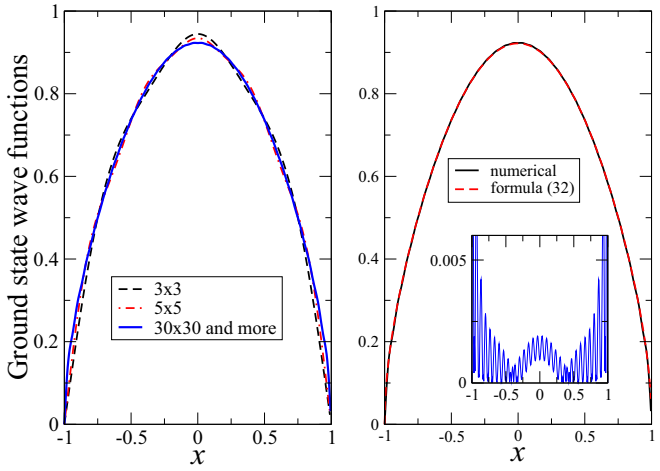

FIG. 2. Left panel. Comparison of the shapes of ground-state functions obtained by the diagonalization of 3×3 (black dashed curve), 5×5 (red dash-dot curve), and 30×30 (blue solid curve) matrices. The shape of ground state functions for matrices more then 30×30 are identical to that for 30×30. Right panel shows the approximation of ground state wave function (for 700×700 matrix, solid curve) by Eq. (41) (dashed curve). As both lines are indistinguishable in the scale of the figure, the inset depicts the modulus of the point-wise difference of respective curves

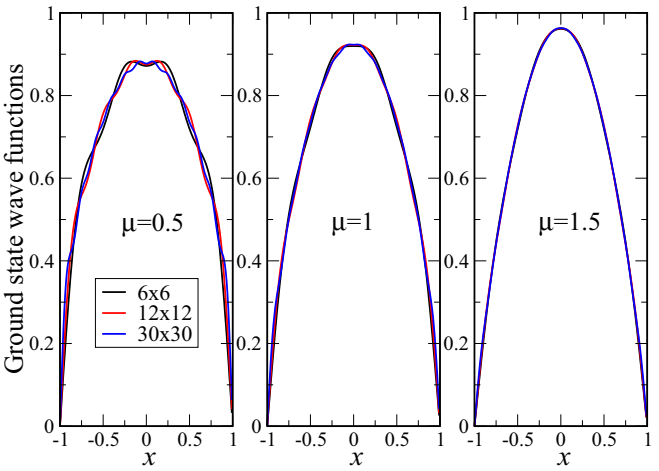

FIG. 3. Ground-state wave functions for different Lévy index μ, obtained for 6×6, 12×12, and 30×30 matrices.

for matrices of sizes exceeding 30×30. This statement is also valid for general case $\mu \neq 1$.

In Ref. [26], an analytic approximation of the ground-state function of $|\Delta|_D^{1/2}$ (i.e., that for $\mu = 1$) has been proposed in the form

$$\psi_1(x) = \psi_{\text{g.s.}}(x) = 0.921749\sqrt{(1-x^2)\cos\alpha x},$$
$$\alpha = \frac{1443\pi}{4096}. \tag{41}$$

In the right panel of Fig. 2, we compare the ground-state function Eq. (41) with that obtained by the diagonalization of 700×700 matrix (which turns out to be close to that obtained by means of the 30×30 matrix; see Fig. 4). It is seen that both functions are indistinguishable within the scale of the figure. The inset in Fig. 2 depicts the modulus of the point-wise difference of these functions. Interestingly, although the approximation is nonmonotonous (the difference oscillates), in a large portion of the interval $-1 \leqslant x \leqslant 1$ the difference does not exceed 0.005.

The ground-state wave functions for different μ's and obtained from the diagonalization of 6×6, 12×12, and 30×30 matrices are reported in Fig. 3. It is seen that the closer μ to 2 (ordinary Laplacian), the faster is convergence. Namely, while for $\mu = 1.5$ the outcome of the matrix 6×6 is to second decimal place is similar to that for 30×30 matrix, in the case $\mu = 0.5$ the difference is distinguishable in the scale of the figure. This fact shows that as $\mu \to 2$, the number of base functions, "taking part" in the wave-function approximation (i.e., the order of the corresponding matrix) tends to only one, corresponding to that for ordinary quantum mechanical infinite well.

Generally, for the approximate eigenfunction, the function $|\Delta|_D^{\mu/2}\psi(x)$ differs from $E\psi(x)$ and symptoms of convergence are expected with the growth of the matrix size. In Fig. 4 we compare the left- and right-hand sides of the integral Eq. (9) for $\mu = 1$ and show the modulus of their difference.

Left panel of Fig. 4 shows that while the function ψ by itself is smooth, the function $|\Delta|_D^{1/2}\psi$ is "wavy" and diverges at the boundaries. The right panel shows the error $||\Delta|_D^{1/2}\psi - E\psi|$

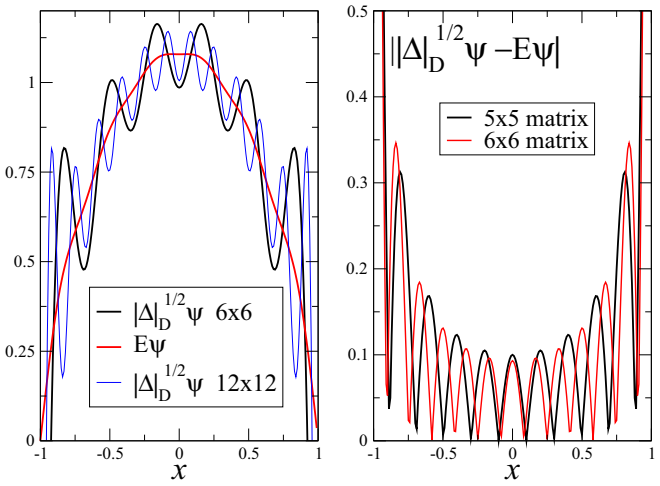

FIG. 4. Left panel, comparison of $|\Delta|_D^{1/2}\psi$ (black curve) and $E\,\psi$ (red curve) for 6×6 matrix. Thin blue line corresponds to 12×12 matrix. It is seen that for the 12×12 matrix $|\Delta|_D^{1/2}\psi$ goes closer to $E\psi$ in the main body of the interval. Right panel, the deviation $||\Delta|_D^{1/2}\psi - E\,\psi|$ for 5×5 (black curve) and 6×6 matrices (red curve).

for 6×6 and 12×12 matrices. It is seen that the divergence at the boundaries is qualitatively the same for both cases, while for the 12×12 matrix the error in the vicinity of $x = 0$ is a little smaller. The same tendence occurs at any $0 < \mu \leqslant 2$. This kind of behavior (slow convergence of $|\Delta|_D^{\mu/2}\psi$ to $E\psi$) is characteristic for integral equations with singular kernels [46] and also for "ordinary" quantum mechanical spectral problems, if we solve them approximately by the expansion method with respect to the full set of eigenfunctions of another operator (here, the Laplacian Δ).

Figure 5 reports the behavior of $E\psi$ and $|\Delta|_D^{1/2}\psi$ for 30×30 and 300×300 matrices. The "wavy" behavior of $A_D\psi$ persists, while $E\psi$ stabilizes already beginning from

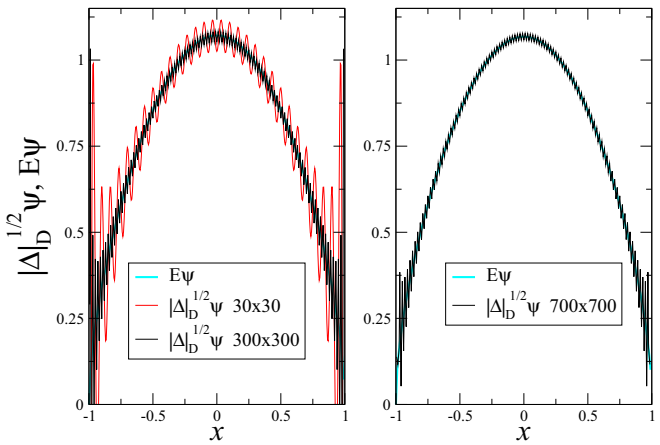

FIG. 5. More detailed comparison of $E\psi$ (cyan curve) and $|\Delta|_D^{1/2}\psi$ (red and black curves) for 30×30 (red curve) and 300×300 (black curve) matrices (left panel). Right panel shows that for matrices larger then 300×300, the "wavy approximation" of $\psi(x)$ approaches (in the adopted scale) the line thickness everywhere, except the close vicinity of $x = \pm 1$ points.

the 12×12 matrix. Our analysis shows that if we take larger matrices, the diverging "tail" moves closer to boundary points ± 1 so that at $n \to \infty$ (n is order of the matrix) it disappears. The same is valid for superimposed oscillations, whose amplitude (slowly) diminishes as n grows. Similar to the situation in Fig. 3, the good convergence for smaller μ's is achieved for larger n. On the other hand, even for relatively small matrices 6×6 we obtain qualitatively reasonable approximations for eigenfunctions and eigenvalues of the operator Eq. (2), especially for indices μ close to 2.

If compared with the previous methods of solution [38,39] and [24,26], our spectral approach seems to be particularly powerful if one is interested in the spectrum of $|\Delta|_D^{\mu/2}$. In fact, we are able to generate an arbitrary number of eigenvalues and corresponding eigenfunctions with any desired accuracy. In Table IV we compare several (first 20 and a couple of larger) lowest eigenvalues of $|\Delta|_D^{1/2}$ (i.e., for typical case $\mu = 1$) and answer how much actually the approximate Eq. (34) deviates from computed E_n's.

It is seen from the Table IV that although the asymptotic formula delivers pretty good approximation to the desirable eigenvalues, the relative error never (except for $n = 11$) falls below $10^{-3}\%$ as the label number n grows. We have actually traced this statement up to $n = 500$. Moreover, the relative error, as it is seen from the Table IV, oscillates around $10^{-3}\%$, which means that beginning with $n \approx 8$, Eq. (34) for $\mu = 1$ contributes five significant digits of the "true" asymptotic answer. Note that for $1 < \mu \leqslant 2$ this number n diminishes so

TABLE IV. The comparison of several eigenvalues of the 5000×5000 matrix Eq. (21) for $\mu = 1$ with the approximate formula $n\pi/2 - \pi/8$ [Eq. (34) at $\mu = 1$] along with the relative error $|E_n - (n\pi/2 - \pi/8)|/E_n$. Independently obtained spectral data (formula (1.11) in Ref. [39]) are displayed as well.

n	$E_{n,5000\times5000}$	Eq. (34)	Rel. error (%)	Data from Ref. [39]
1	1.157791	1.178097	1.75	1.157773
2	2.754795	2.748894	0.21	2.754754
3	4.316864	4.319690	0.06	4.316801
4	5.892233	5.890486	0.03	5.892147
5	7.460284	7.461283	0.013	7.460175
6	9.032984	9.032079	0.01	9.032852
7	10.602447	10.602875	0.004	10.602293
8	12.174295	12.173672	0.0051	12.174118
9	13.744308	13.744468	0.0012	13.744109
10	15.315777	15.315264	0.0033	15.315554
11	16.886062	16.886061	$5.9\cdot10^{-8}$	*
12	18.457329	18.456857	0.0026	*
13	20.027767	20.027653	0.00057	*
14	21.598914	21.598449	0.0021	*
15	23.169448	23.169246	0.00087	*
16	24.740517	24.740042	0.0019	*
17	26.311115	26.310838	0.0011	*
18	27.882131	27.881635	0.0018	*
19	29.452773	29.452431	0.0012	*
20	31.023751	31.023227	0.0016	*
30	46.731898	46.731191	0.0015	*
50	78.148251	78.147117	0.0015	*
100	156.689159	156.686934	0.0014	*

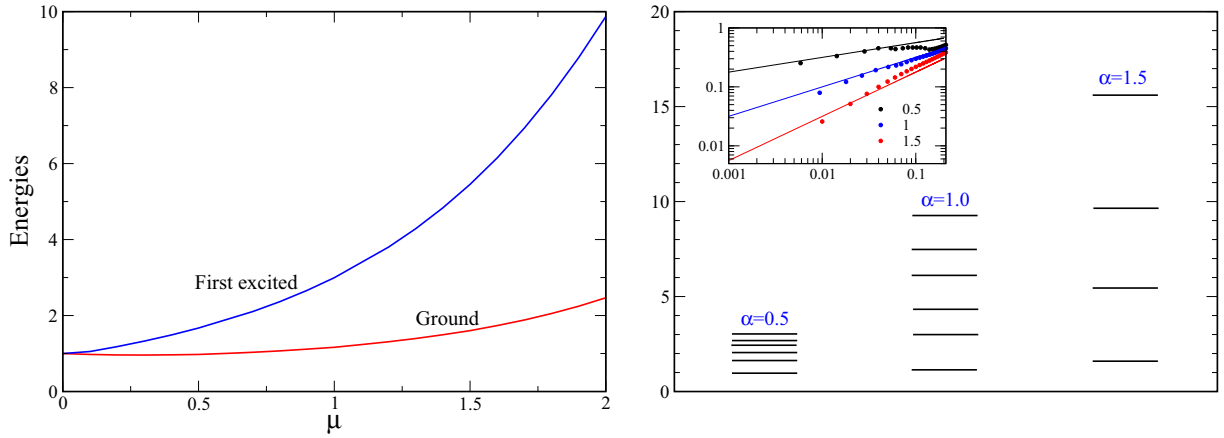

FIG. 6. The properties of the spectrum of integral Eq. (9) for different μ's. Left panel shows the dependence of ground and first excited states energies on the parameter μ. At $\mu = 2$ the energy levels positions are equal to those in the ordinary quantum well Eq. (42). At $\mu = 0$ all spectrum merges into the single level $E_0 = 1$ (in our units). Right panel visualizes how several first energy levels look like for different μ's. The shrinking of the spectrum at $\mu \to 0$ is clearly seen. The inset shows in double log plot the character of decay of ground-state wave functions at $x = \pm 1$. For better visualization we shift the left part of the functions (i.e., those at $x = -1$) to zero. Points report the wave functions and lines are $(x+1)^{\mu/2}$ for $\mu = 0.5$, 1 and 1.5, respectively.

that at $\mu = 1.9$ the same result is obtained already for $n = 2$. On the other hand, at $\mu = 0.2$ for $n = 50$ we have only three significant digits.

Although the numerical calculations for the case $\mu = 1$ are (sometimes much) less computer intensive then those for $\mu \neq 1$, the former case does not permit to trace the additional properties of the spectrum of Eq. (9), which depend on μ. These properties are summarized in Fig. 6. In the left panel we plot the μ dependence of ground and first excited state energies. All other energies are also available, but their values at $\mu = 2$ grow rapidly with n so that for higher excited states not all μ's will fit the scale of the plot. This is because at $\mu = 2$ the spectrum of Eq. (9) gives exactly that for ordinary quantum well [41], which in our units has the form

$$E_{n,\mu=2} = \frac{\pi^2}{4} n^2,\ n = 1,2,3,..., \tag{42}$$

i.e., it is proportional to n^2. Note that at $\mu = 2$ the approximate dependence Eq. (34) yields exactly Eq. (42), thus also giving exact known result.

Substituting $n = 1$ and 2 into Eq. (42) we have, respectively, $E_{1,\mu=2} = \pi^2/4 \approx 2.4674$ and $E_{2,\mu=2} = \pi^2 \approx 9.8696$, which are seen in the left panel of Fig. 6 at $\mu = 2$. For instance, at $n = 3$ $E_{3,\mu=2} = 9\pi^2/4 \approx 22.2066$, which is two times larger then $E_{2,\mu=2}$.

The most interesting feature of our method is that it permits us to transit smoothly to the case $\mu = 0$, which does not included in the domain of the operator Eq. (2). Moreover, the integral Eqs. (16) and (36) can be exactly evaluated in this case. This gives explicitly

$$f_{k,\mu=0} = \cos \lambda_k x,\ g_{k,\mu=0} = \sin b_k x, \tag{43}$$

which, in turn, yields

$$\gamma_{\mu=0,ki} = \eta_{\mu=0,ki} = \delta_{ki}. \tag{44}$$

Equation (44) immediately shows that at $\mu = 0$ all eigenvalues of Eq. (9) are equal to 1. In other words, the entire spectrum of the operator Eq. (2) at $\mu = 0$ shrinks into one single value $E_0 = 1$. This value is seen on the left panel of Fig. 6.

The character of spectrum shrinking at $\mu \to 0$ is shown on the right panel of Fig. 6. Here we report several first energy levels for different μ's. The expansion of the spectrum as $\mu \to 2$ and its shrinking as $\mu \to 0$ is clearly seen.

An important feature of the eigenfunctions of the operator Eq. (2) is that, contrary to trigonometric functions for $\mu = 2$, they decay nonlinearly at $x = \pm 1$. The hypothesis is that they vanish as $(1 \pm x)^{\mu/2}$. To check this hypothesis, in the inset to right panel of Fig. 6 we plot (shifting for convenience the left edge $x = -1$ to zero) the ground-state wave functions (points) for different μ's along with functions $(1+x)^{\mu/2}$ in double logarithmic scale (full lines). It is seen that at $0.01 < x < 0.1$ the coincidence is almost perfect. However, small deviations are seen already at $x = 0.01$. This is related to the approximate character of wave functions. To continue the points to smaller x, the consideration of larger matrices is necessary, which (even for eigenvectors of large matrices, corresponding to $\mu = 1$) is an extremely computer intensive task. Most probably, the hypothesis about asymptotics $(1 \pm x)^{\mu/2}$ is true.

IV. CONCLUSIONS

In the present paper we have studied the spectrum of the problem of a particle in the infinite potential well, obeying fractional quantum mechanics with arbitarary Lévy index $0 < \mu \leqslant 2$. This problem is relevant to many disordered and dissipative physical (and biological, chemical, and even social) systems, involving Lévy flights in bounded domains and is nontrivial as the familiar representation of fractional derivatives in Fourier domain does not work in such confined case. To solve this problem, we reduce the initial fractional Schrödinger equation to the Fredholm integral equation with hypersingular kernel. For the solution of the latter equation, we have elaborated a novel and powerful method, based on the expansion over the complete set of the orthogonal functions taken from corresponding "ordinary" quantum mechanical

problem for Lévy index $\mu = 2$. In our case of the interval $-1 \leqslant x \leqslant 1$ we use the trigonometric functions, which are eigenfunctions of the ordinary Laplacian. We note here the general character of our method in the sense of its applicability to virtually any "ordinary" quantum mechanical problem, also in two and three dimensions.

Let us finally mention the realistic physical systems, where we are going to apply our formalism. One of the important examples is electronic tunneling characteristics in spintronic devices [49–51]. Spintronics or spin electronics is nowadays a branch of physics whose central theme is the active manipulation of spin degrees of freedom in solid-state systems [49,52,53]. It is widely believed that spintronic devices can lead to applications (like quantum computers) that are so far infeasible with modern electronics. Despite intense experimental and theoretical studies, the statistics of tunneling electrons through barriers in such structures remains unclear due to disorder, which is inevitably present in such structures [52,53]. The above barriers are technologically realized in inversion semiconductor layers, heterostructures (like perovskite interface $LaAlO_3$-$SrTiO_3$ [54–56]), quantum wells, or in graphene [52,53,57]. The common formalism for description of electronic states in the above structures is different variations of particle in a potential well problem (see, e.g., Ref. [58] and references therein). It has been suggested that to describe the tunneling statistics adequately, the fractional derivatives should be brought into the above formalism. We are going to apply the developed formalism to the "disordered" quantum wells as well as to oxide interfaces [54,55], which also has interesting and nontrivial physical properties. One more problem is the electronic properties of so-called multiferroics, i.e., substances combining several types of long-range orders (such as ferroelectricity and ferromagnetism). The non-Gaussian statistics due to disorder plays an important role in these substances also [59,60] and we are applying now our formalism (also in context of the problem of quantum oscillator with fractional Laplacian) to obtain the adequate description of their physical properties.

[1] *Lévy Flights and Related Topics in Physics*, edited by M. F. Shlesinger, G. M. Zaslavsky, and U. Frisch, Lecture Notes in Physics (Springer-Verlag, Berlin, 1995).

[2] B. D. Hughes, *Random Walks and Random Environments*, Vol. 1 (Clarendon Press, Oxford, 1995).

[3] *Chaos: The Interplay Between Deterministic and Stochastic Behavior*, edited by P. Garbaczewski, M. Wolf, and A. Weron (Springer-Verlag, Berlin, 1995).

[4] B. V. Gnedenko and A. N. Kolmogorov, *Limit Distributions for Sums of Random Variables* (Addison-Welsey, Reading, MA, 1954).

[5] A. A. Dubkov, B. Spagnolo, and V. V. Uchaikin, Int. J. Bifurcat. Chaos **18**, 2649 (2008).

[6] R. Metzler and J. Klafter, Phys. Rep. **339**, 1 (2000).

[7] G. M. Zaslavsky. *Hamiltonian Chaos and Fractional Dynamics* (Oxford University Press, New York, 2005).

[8] D. del-Castillo-Negrete, B. A. Carreras, and V. E. Lynch, Phys. Rev. Lett. **91**, 018302 (2003).

[9] B. Bergersen and Z. Racz, Phys. Rev. Lett. **67**, 3047 (1991).

[10] S. Schaufler, W. P. Schleich, and V. P. Yakovlev, Phys. Rev. Lett. **83**, 3162 (1999).

[11] A. Carati, L. Galgani, and B. Pozzi, Phys. Rev. Lett. **90**, 010601 (2003).

[12] G. M. Viswanathan, V. Afanasyev, S. V. Buldyrev, E. J. Murphey, P. A. Prince, and H. E. Stanley, Nature **381**, 413 (1996).

[13] E. N. Govorun, V. A. Ivanov, A. R. Khokhlov, P. G. Khalatur, A. L. Borovinsky, and A. Y. Grosberg, Phys. Rev. E **64**, 040903 (2001).

[14] N. Scafetta, V. Latora, and P. Grigolini, Phys. Rev. E **66**, 031906 (2002).

[15] R. N. Mantegna and H. E. Stanley, *An Introduction to Econophysics. Correlations and Complexity in Finance* (Cambridge University Press, Cambridge, 2000).

[16] W. Schoutens, *Lévy Processes in Finance* (Wiley Finance, New York, 2003)

[17] S. Rachev, Y. Kim, M. Bianchi, F. Fabozzi, *Financial Models with Lévy Processes and Volatility Clustering* (Wiley, New York, 2011).

[18] V. I. Fal'ko, K. B. Efetov, Phys. Rev. B **52**, 17413 (1995).

[19] A. Mildenberger, A. R. Subramaniam, R. Narayanan, F. Evers, I. A. Gruzberg, and A. D. Mirlin, Phys. Rev. B **75**, 094204 (2007).

[20] A. Saichev and G. M. Zaslavsky, Chaos **7**, 753 (1997).

[21] I. Podlubny, *Fractional Differential Equations* (Academic Press, London, 1999).

[22] S. G. Samko, A. A. Kilbas, and O. I. Maritchev, *Fractional Integrals and Derivatives* (Gordon and Breach, New York, 2003).

[23] P. Garbaczewski and V. Stephanovich, J. Math. Phys. **54**, 072103 (2013).

[24] M. Żaba and P. Garbaczewski, J. Math. Phys. **55**, 092103 (2014).

[25] P. Garbaczewski and M. Żaba, Acta Phys. Pol. B **46**, 231 (2015).

[26] M. Żaba and P. Garbaczewski, J. Math. Phys. **56**, 123502, (2015).

[27] P. Garbaczewski and R. Olkiewicz, J. Math. Phys. **40**, 1057 (1999).

[28] A. Zoia, A. Rosso, and M. Kardar, Phys. Rev. E **76**, 021116 (2007).

[29] R. K. Getoor, Trans. Amer. Math. Soc. **101**, 75 (1961).

[30] P. Garbaczewski and V. A. Stephanovich, Phys. Rev. E **80**, 031113 (2009).

[31] P. Garbaczewski and V. A. Stephanovich, Phys. Rev. E **84**, 011142 (2011).

[32] A. V. Chechkin, V. Yu. Gonchar, J. Klafter, and R. Metzler, Adv. Chem. Phys. **133**, 439 (2006).

[33] S. V. Buldyrev, S. Havlin, A. Ya. Kazakov, M. G. E. da Luz, E. P. Raposo, H. E. Stanley, and G. M. Viswanathan, Phys. Rev. E **64**, 041108 (2001).

[34] Y. Luchko, J. Math. Phys. **54**, 012111 (2013).

[35] A. Iomin, Chaos, Solitons Fractals **71**, 73 (2015).

[36] M. Riesz, Acta Math. **81**, 1 (1949).

[37] J. Hadamard, *Lectures on Cauchy's Problem in Linear Partial Differential Equations* (Dover, New York, 1952).

[38] M. Kwaśnicki, J. Funct. Anal. **262**, 2379 (2012).
[39] T. Kulczycki, M. Kwaśnicki, J. Małecki, and A. Stós, Proc. London. Math. Soc. **101**, 589 (2010).
[40] B. Dyda, Colloquium Math. **122**, 59 (2011).
[41] L. D. Landau and E. M. Lifshits, *Quantum Mechanics. Nonrelativistic Theory* (Pergamon Press, Oxford, 1995).
[42] E. M. Stein, *Singular Integrals and Differentiability Properties of Functions* (Princeton University Press, Princeton, 1970).
[43] A. C. Kaya and F. Erdogan, Quart. Appl. Math. **45**, 105 (1987).
[44] W. T. Ang, *Hypersingular Integral Equations in Fracture Analysis* (Woodhead Publishing, Cambridge, 2013).
[45] Y.-S. Chan, A. C. Fannjiang and G. H. Paulino, Int. J. Eng. Sci. **41**, 683 (2003).
[46] A. D. Polyanin and A. V. Manzhirov, *Handbook of Integral Equations* (Chapman & Hall/CRC Press, Boca Raton-London, 2008).
[47] I. S. Gradshteyn and I. M. Ryzhik, *Table of Integrals, Series, and Products*, 8th ed., edited by Daniel Zwillinger and Victor Moll (Academic Press, London, 2014).
[48] *Handbook of Special Functions*, edited by M. Abramowitz and I. A. Stegun (National Bureau of Standards, NY, 1964).
[49] I. Žutić, J. Fabian, S. Das Sarma, Rev. Mod. Phys. **76**, 323 (2004).
[50] Y. Yamauchi, K. Sekiguchi, K. Chida, T. Arakawa, S. Nakamura, K. Kobayashi, T. Ono, T. Fujii, and R. Sakano, Phys. Rev. Lett. **106**, 176601 (2011).
[51] T. D. Nguyen, E. Ehrenfreund, and Z. V. Vardeny, Science **337**, 204 (2012).
[52] A. H. Castro Neto, F. Guinea, N. M. R. Peres, K. S. Novoselov, and A. K. Geim, Rev. Mod. Phys. **81**, 109 (2009).
[53] S. Das Sarma, S. Adam, E. H. Hwang, and E. Rossi, Rev. Mod. Phys. **83**, 407 (2011).
[54] A. Ohtomo and H. Y. Hwang, Nature **427**, 423 (2004).
[55] V. A. Stephanovich, V. K. Dugaev and J. Barnaś, Phys. Chem. Chem. Phys. **18**, 2104 (2016).
[56] V. A. Stephanovich and V. K. Dugaev, Phys. Rev. B **93**, 045302 (2016).
[57] A. K. Geim and K. S. Novoselov, Nat. Mater. **6**, 183 (2007).
[58] S. M. Sze and K. K. Ng, *Physics of Semiconductor Devices*, 3rd ed. (John Wiley and Sons, Hoboken, NJ, 2007).
[59] V. V. Laguta, V. A. Stephanovich, M. Savinov, M. Marysko, R. O. Kuzian, I. V. Kondakova, N. M. Olekhnovich, A. V. Pushkarev, Yu. V. Radyush, I. P. Raevski, S. I. Raevskaya and S. A. Prosandeev, New J. Phys. **16**, 113041 (2014).
[60] V. A. Stephanovich and V. V. Laguta, Phys. Chem. Chem. Phys. **18**, 7229 (2016).